

SLAC-PUB-616  
June 1969  
(EXP)

A STUDY OF HYPERON-NUCLEON INTERACTION IN  
THE REACTION:  $K^-D \rightarrow \pi^- p \Lambda$  AT REST\*

Tai Ho Tan

Stanford Linear Accelerator Center  
Stanford University, Stanford, California 94305

ABSTRACT

A  $\Lambda p$  system with high statistics and mass resolution was studied in detail. The broad bump in the low mass region can be attributed to contribution from both the impulse and final state interaction mechanisms. The low energy  $\Lambda p$  scattering parameters are deduced to be  $a_0 = -2.0 \pm .5$  and  $r_0 = 3.0 \pm 1.0$  fermi. The higher mass spectrum can be fitted to two Breit-Wigner resonant structures with  $M_1 = 2128.7 \pm .2$ ,  $\Gamma_1 = 7.0 \pm .6$ , and  $M_2 = 2138.8 \pm .7$ ,  $\Gamma_2 = 9.1 \pm 2.4$  MeV. Attempts were carried out to understand these peaks via a  $\Sigma N$  final state interaction model.

(Submitted to Phys. Rev. Letters)

---

\* Work supported by the U. S. Atomic Energy Commission.

An experiment to investigate hyperon nucleon production in  $K^-D$  interaction at rest was carried out by exposing the Columbia-BNL 30-inch deuterium bubble chamber to a low energy separated  $K^-$  beam at the AGS. We present here results from the study of reaction  $K^-D \rightarrow \pi^- p \Lambda$ . A detailed analysis on a precisely measured  $\Lambda p$  mass spectrum was carried out with the aid of a final state hyperon-nucleon interaction model as is schematically represented by the diagram in Fig. 1. In particular, we have attempted to determine the nature of the observed enhancement near the 2129 MeV region<sup>1-3</sup> and to extract information on  $\Lambda p$  and  $\Sigma^+ n$  scatterings.

Our data includes 2470 events from sample (a) where all particles were measured and 2431 events from sample (b) where  $\Lambda$  was missing. All events from (a) satisfied a two vertex 7C fit while events from (b) satisfied a 1C fit. No ambiguity in the fit between  $\Lambda$  and  $\Sigma^0$  production was found. To minimize the measurement errors a fiducial volume was imposed to ensure that at least 10 cm of measurable track length is available for all nonstopping charged tracks. Events with a stopping proton track length of less than 1 mm or with a secondary scattering were discarded. Chances of any systematic shift in the mass distribution was reduced by a careful study of the chamber magnetic field and the range-momentum relationship.

Figure 2 exhibits the distribution of events in the two-dimensional mass plot,  $M(\Lambda p)$  vs  $M(\Lambda \pi^-)$ . Obvious evidence of structures in the  $\Lambda p$  mass system appears both in the low mass region and at around 2130 MeV, while no significant amount of  $Y^*(1385)$  appears to be in evidence. No strong formation of any  $I = 1/2 \pi^- p$  system is observed nor is it expected in the allowed mass region. Gaussian ideogram of events projected on the  $\Lambda p$  mass axis is shown in Fig. 3a.

The distribution contains events from both samples (a) and (b). The average mass resolution from the two samples are 1.0 MeV and 2.6 MeV, respectively. It features a broad clustering of events in the low mass region, a striking enhancement with an apparent narrow width at about 2129 MeV, and a shoulder that protrudes out to about 2140 MeV.

We have investigated the directional angular distribution of  $\Lambda$  in the rest frame of  $\Lambda p$  system with respect to the intermediate hyperon, opposite to the  $\pi^-$  direction, as well as the polarization of the  $\Lambda$ . Figures 3c and 3d show the forward-backward and the polar-equatorial distribution of the  $\Lambda$ -direction as a function of  $\Lambda p$  mass. Figure 3e exhibits the up-down distribution of the decay pion from  $\Lambda$  with respect to the normal to  $\Lambda$ -intermediate hyperon plane.

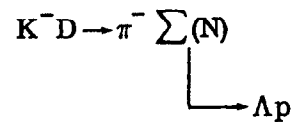
A detailed study of  $\Lambda \pi$ -mass system and its angular distribution indicates the presence of some  $Y^*(1385)$ . The maximum estimated reflection from these events on the  $\Lambda p$  mass spectrum can be represented by the dashed curve drawn on Fig. 3a.<sup>4</sup> Since  $Y^*$  state is  $P^{3/2}$  and  $K^- \Lambda$  parity is odd, the recoil proton must be produced in an odd angular momentum state with respect to  $Y^*$ . The consequent reflection produces asymmetry in both the directional angular correlation and polarization distribution in the  $\Lambda p$  system, especially in the region between 2070 to 2110 MeV where the signal of  $Y^*$  is expected to be dominant.

In an attempt to understand the remainder of the events in the  $\Lambda p$  system we followed the final state interreaction formalism developed in Refs. 5 and 6. Using this model, information about hyperon-nucleon interaction can be extracted. This is so because the other two vertices in the diagram are known. The amplitude at the deuteron vertex can be represented by the Huthlén wave function and the parameters describing the low energy  $\bar{K}N$  scattering have been obtained by Kim.<sup>7</sup> Furthermore, if hyperon-nucleon interaction at low energy is

dominated by S-wave, then  $\Lambda p$  system will be produced in the same state as the deuteron, i. e., a  $^3S$  state. Impulse contribution in the case where final state interaction does not occur is contained in the model.

In order to describe the spectrum in the low mass region, we found that contribution from both the direct production process  $K^- n(p) \rightarrow \pi^- \Lambda(p)$  and the final state  $\Lambda$ -p interaction process were necessary. Direct  $\Lambda$  production accounts for about two-thirds of the events. If S-wave effective range approximation is assumed for  $\Lambda p$  interaction, we deduced  $a_0 = -2.0 \pm .5$  and  $r_0 = 3.0 \pm 1.0$  fermi, where  $a_0$  is the zero energy scattering length and  $r_0$  is the effective range. This is in very good agreement with the triplet parameters obtained from the study of direct  $\Lambda p$  scattering.<sup>8</sup> The deviation of both the directional angular correlation and the polarization distribution from isotropy can be ascribed to the presence of directly produced  $\Lambda$  events.

In the region near and above the threshold of  $\Sigma N$  rest mass, we have investigated the  $\Lambda p$  spectrum via a two step process<sup>9</sup>



The result of the calculation is compared with Fig. 3b which includes only the higher resolution sample. We have included in the matrix element contribution from the intermediate  $\Sigma^+$  and  $\Sigma^0$  diagrams as well as the interference term. By assuming charge symmetry in  $\Sigma^+ n$  and  $\Sigma^0 p$  scattering, we estimated that the contribution from  $\Sigma^0$  diagram is less than one-seventh the contribution from  $\Sigma^+$  diagram. We found that the  $\Sigma^0$  contribution approximately cancels out the contribution from the interference term. The effect of  $\Sigma^+ - \Sigma^0$  mass difference is included in the consideration.

At  $\Sigma^+n$  threshold, the directional angular distribution of  $\Lambda$  is isotropic and  $\Lambda$  is also observed to be unpolarized. This is consistent with S-wave  $\Sigma N$  scattering. In the zero range approximation, the enhancement can be described by the complex scattering length  $\underline{a} + i\underline{b}$ . The rate of production depends primarily on  $\underline{b}$ , while the shape and the center of the enhancement are very sensitive to the sign and the value of  $\underline{a}$ . If we neglect the fact that the intermediate  $\Sigma$  and  $N$  are both off the mass shell, then the complex scattering length  $(0.8 - 1.8i)$  fermi will provide a good fit to the shape of the peak as is indicated by the solid line in Fig. 3b. However, such a small positive value of  $\underline{a}$  would imply a large binding energy, in the order of  $(2\mu_{\Sigma N} \underline{a}^2)^{-1} \approx 59$  MeV, which grossly disagrees with the data. The center of the peak is at most only a few tenths of an MeV below the  $\Sigma^+N$  threshold. If the off-mass shell effects are taken into account the effective  $\Sigma N$  threshold mass is shifted lower. Subsequently, a negative  $\underline{a}$  will be needed to describe the peak. A preliminary analysis of the  $\Sigma^+n$  system from the reaction  $K^-D \rightarrow \pi^- \Sigma^+n$  without any off-mass shell correction also appears to support a similar conclusion. This would imply that within the present framework the observed  $\Lambda p$  enhancement is not a bound state of  $\Sigma^+n$  system. It is clear that proper consideration of the off-mass shell effect must be done before a meaningful set of complex scattering length can be deduced. Furthermore, we have not included in the above analysis the possible contribution from an intermediate  $\Lambda$  diagram. Such an addition may alter the conclusion substantially. However, this can be done reliably only after sufficient information about  $\Lambda p$  interaction is known.

It is not clear at the moment whether or not the excess of events in the 2140 MeV region has any physical significance, although the shoulder becomes more prominent when the number of events is increased by a factor of 2

(see Fig. 3a). We have attempted to reproduce the shoulder by introducing an effective range term into  $\underline{a}$ . Under our present scheme, no satisfactory solution has been obtained.<sup>10</sup> Both the forward-backward and up-down distribution indicate a possible asymmetry of about 0.16 in this region. It is worth pointing out that a similar amount of asymmetry was reported in the study of the reaction  $\Sigma^- p \rightarrow \Lambda n$  at around 160 MeV/c.<sup>11</sup> The effect may therefore be due to the presence of  $\ell \neq 0$  higher order partial wave states.

We have chosen also to fit the distribution in Fig. 3a to a Breit-Wigner resonant function and a slowly varying background. Two resonances are found to be necessary to describe the spectrum. The fitted shape parameters for the two resonances are:  $M_1 = 2128.7 \pm .2$ ,  $\Gamma_1 = 7.0 \pm .6$ , and  $M_2 = 2138.8 \pm .7$ ,  $\Gamma_2 = 9.1 \pm 2.4$  MeV. The fitted curve is shown in Fig. 3a. An identical fit was obtained also from Fig. 3b. The closeness of the first peak to the  $\Sigma^+ n$  threshold makes it impossible to distinguish between a possible genuine  $\Lambda p$  resonant state that may exist a fraction of an MeV below the  $\Sigma N$  threshold from a threshold cusp effect. It is entirely possible that the observed peak is a superposition of both. It is worth mentioning that an analysis of  $\Lambda$ -N interaction inside the hypernuclei via a potential model indicates the existence of a  $({}^3S_1 - {}^3D_1)$   $\Lambda$ -N resonance with a mass positioned about 0.05 MeV below the  $\Sigma^+ n$  threshold.<sup>12</sup> Confirmation of this, as well as further interpretation of the above observed peaks, must await more data from direct  $\Lambda N$  and  $\Sigma N$  scatterings.

#### ACKNOWLEDGEMENTS

The author wished to express appreciation to Professor Martin Perl for support, to the scanning crew for their careful and diligent efforts, to the 30-inch bubble chamber crew at BNL for their fine work during the exposure, to Dr. D. Berley for the use of his excellently designed beam transport system, and to Professor B. Downs for illuminating discussions.

## LIST OF REFERENCES

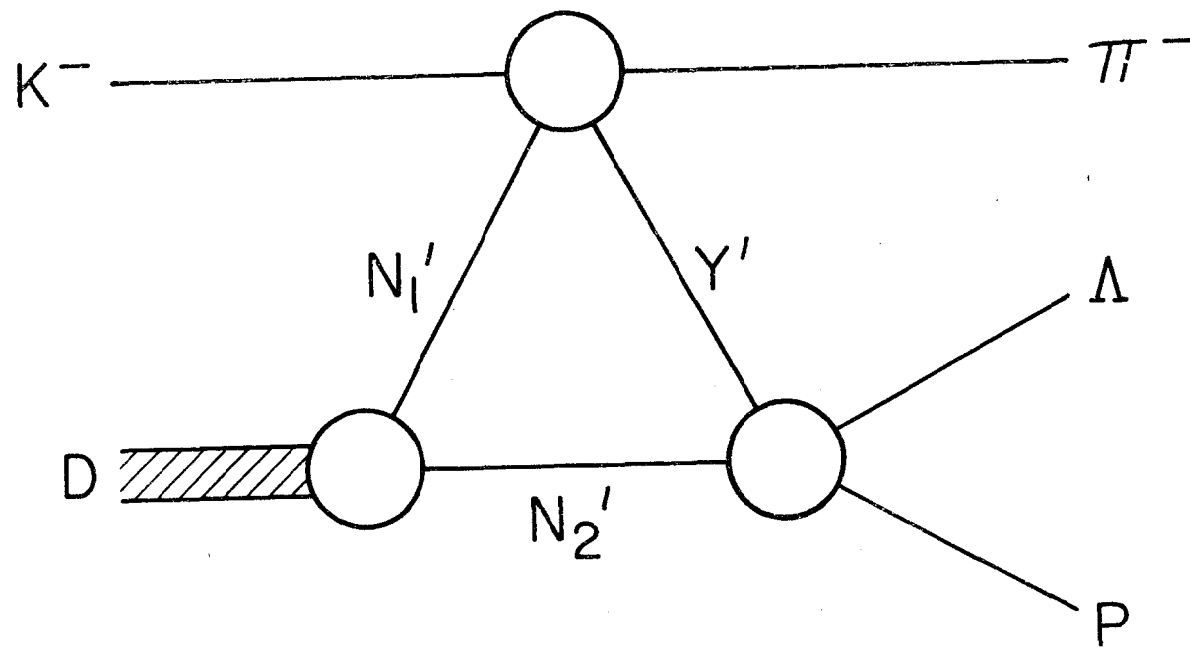
1. O. Dahl et al., Phys. Rev. Letters 6, 142 (1961).
2. D. Cline et al., Phys. Rev. Letters 3, 1452 (1969).
3. G. Alexander et al., Phys. Rev. Letters 22, 483 (1968)
4. If we take the density of the  $Y^*$  band from the region between 2080 to 2100 MeV in the  $\Lambda p$  system and the density in the  $\Lambda p$  (2129) band to be represented by the region below 1350 in the  $\Lambda \pi^-$  system, then we found that the population density inside the overlapped area is equal to the incoherent sum of the two. Therefore, we do not have to be concerned with possible interference effect, and the true population density for the  $Y^*$  band may be assumed uniform.
5. R. Karplus and L. Rodberg, Phys. Rev. 115, 1058 (1959).
6. T. Kotani and M. Ross, Nuovo Cimento XIV, 1282 (1959).
7. J. K. Kim, Phys. Rev. Letters 14, 29 (1965).
8. G. Alexander et al., Phys. Rev. 173, 1452 (1968).
9. Comparison with the preliminary data from  $\pi^- \Sigma^0 p$  and  $\pi^- \Sigma^+ n$  reactions indicates that the ratio of the inelastic to elastic channels is close to unity. This supports the conjecture that  $K^- D$  interaction at rest is dominated by the final state interaction mechanism.
10. If a sufficiently large value of effective range is employed (about 14 fermis) the scattering length formalism can provide two resonant structures, i. e., a narrow peak at around 2128.7 MeV and a broader peak at around 2138 MeV. However, the maximum height of the second peak is limited by the zero effective range solution. Therefore, it cannot account for the excess events.
11. R. Engelmann et al., Phys. Letters 21, 587 (1966).

12. B. W. Downs, talk delivered at the International Conference on Hypernuclei, Argonne National Laboratory, Argonne, Illinois, (May 5-7, 1969). (To be published in the proceedings.) In their model, the  $\Lambda_p$  resonance can be distinctly separated from the  $\Sigma^+ n$  threshold cusp effect. (Recent private communication.)



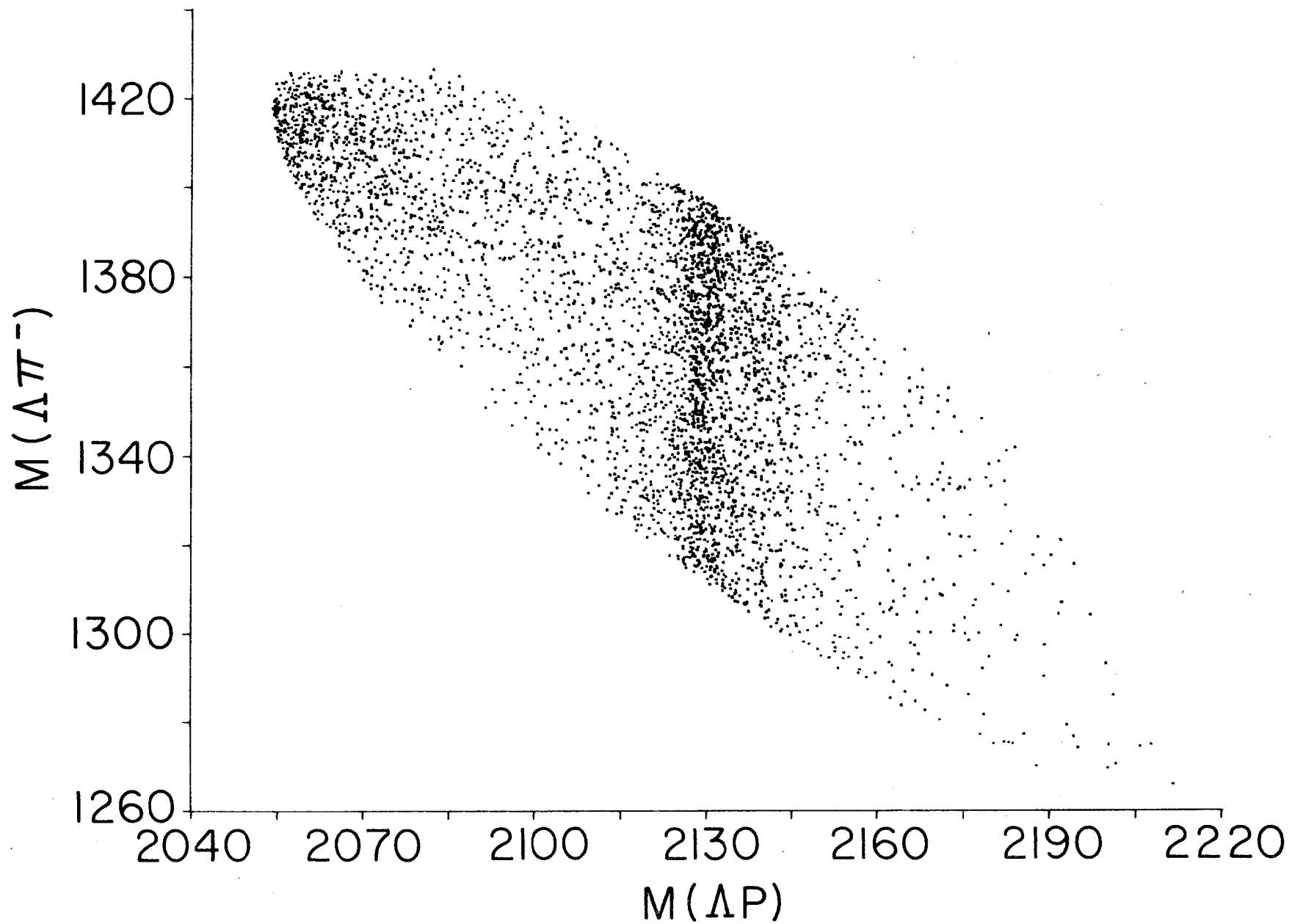
## FIGURE CAPTIONS

1. Schematic diagram showing final state hyperon-nucleon interaction.
2. "Dalitz Plot"  $M(\Lambda \pi^-)$  vs  $M(\Lambda p)$ .
3. a)  $\Lambda p$  combined mass ideogram for all events.  
b) Ideogram showing the distribution in higher mass region for events from sample (a)  
c)  $\Lambda$  angular distribution in the form  $(F-B)/(F+B)$  is a function of  $\Lambda p$  mass.  
d) Plotted as  $(P-E)/(P+E)$ .  
e) Decay  $\pi^-$  angular distribution with respect to axis normal to  $\Lambda$  production plane.



1277A14

Fig. 1



1277A8

Fig. 2

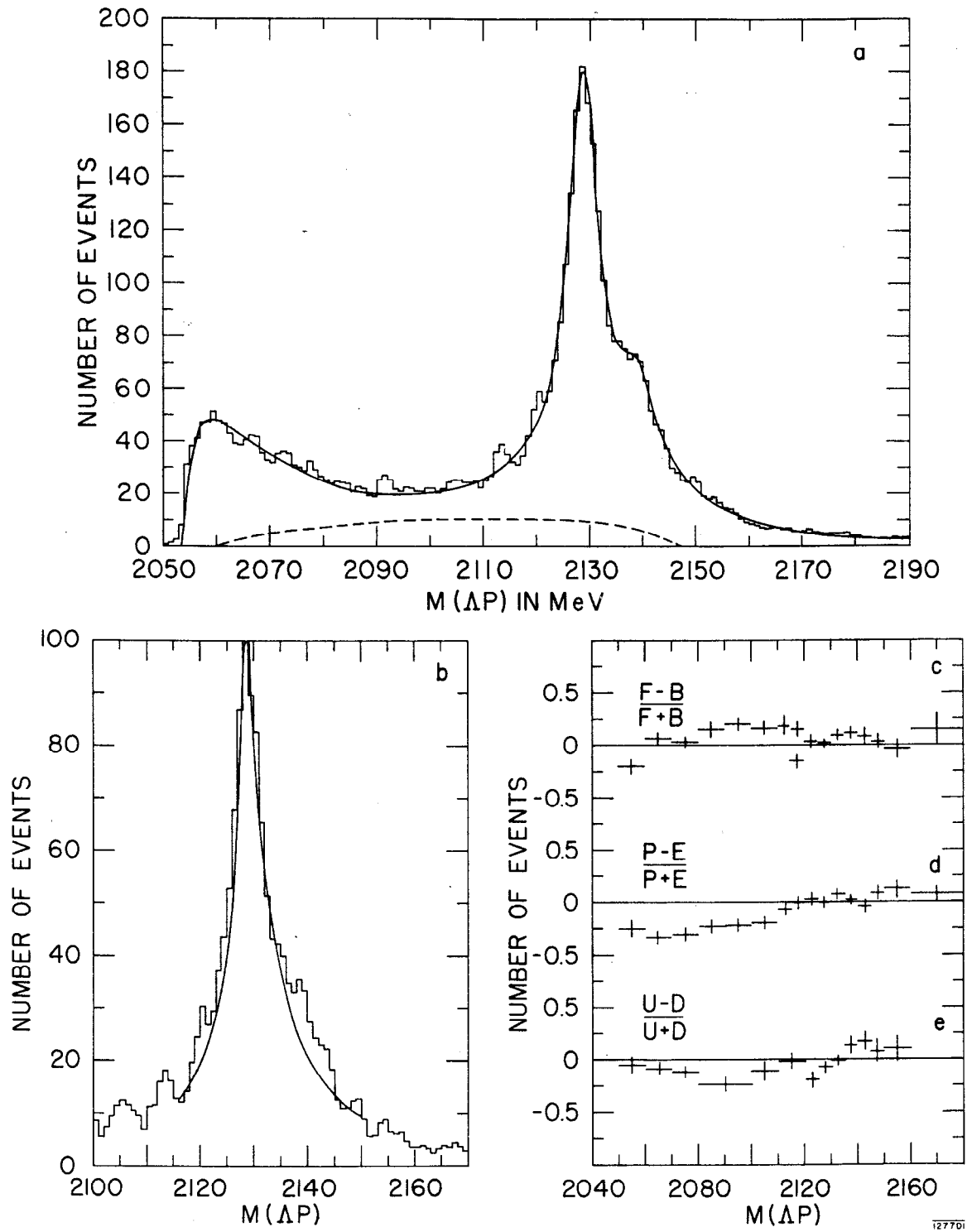


Fig. 3